Supporting Information

Protein Uptake into Individual Hydrogel Microspheres Visualized by High-Speed Atomic Force Microscopy

Shusuke Matsui,[a] Kensuke Hosho,[a] Haruka Minato,[a] Takayuki Uchihashi*[c] and Daisuke Suzuki*[ab]

[a]Graduate School of Textile Science & Technology, Shinshu University
[b]Research Initiative for Supra-Materials, Interdisciplinary Cluster for Cutting Edge Research, Shinshu University, 3-15-1 Tokida, Ueda, Nagano 386-8567, Japan
[c]Department of Physics and Structural Biology Research Center, Graduate School of Science, Nagoya University, Furo-cho, Chikusa-ku, Nagoya, Aichi 464-8602, Japan, and Exploratory Research Center on Life and Living Systems, National Institutes of Natural Sciences, 5-1 Higashiyama, Myodaiji, Okazaki, Aichi, 444-8787, Japan

*Author to whom correspondence should be addressed.
E-mail: d_suzuki@shinshu-u.ac.jp (D.S.), uchihast@d.phys.nagoya-u.ac.jp (T.U.)

Experimental Section

Materials

N-isopropyl acrylamide (NIPAm, 98%), *N*,*N*′-methylenebis(acrylamide) (BIS, 97%), sodium dodecyl sulfate (SDS, 95%), potassium persulfate (KPS, 95 %), disodium hydrogen phosphate (Na_2HPO_4, 99%), sodium dihydrogen phosphate (NaH_2PO_4, 98%), lysozyme (LZM), avidin (Avi), immunoglobulin G (IgG), and the protein assay bicinchoninic acid (BCA) kit were purchased from Wako Pure Chemical Industries (Japan) and used as received. Acrylic acid (AAc, 99%), was purchased from SIGMA-ALDRICH and used as received. Fluoride resin (Fluoro Surf) was purchased from Fluoro Technology (Japan) and used as received. Water for all reactions, the preparation of solutions, and the purification of polymers was distilled and ion-exchanged (EYELA, SA-2100E1).

Microgel synthesis

PolyNIPAm (**Scheme S1(a)**: **N**) microgels were synthesized through aqueous free-radical precipitation polymerization. A monomer mixture of NIPAm (8.402 g, 99 mol%), BIS cross-linker (0.116 g, 1 mol%) in water (485 mL) was poured into a three-necked, round-bottom flask (1000 mL) which is equipped with a mechanical stirrer, condenser, and nitrogen gas inlet. The monomer solution was heated to 70 °C in an oil bath under nitrogen sparging (30 min) and constant stirring (250 rpm). After 30 min, to initiate the polymerization, SDS (0.144 g, 1 mM) dissolved in water (10 mL) and the KPS initiator (0.270 g, 2 mM) dissolved in water (5 mL) were injected into the flask. Thereafter 4 h, the dispersion was cooled to room temperature to stop the reaction. The obtained microgels were purified via two cycles of centrifugation (415,000×g at 15 °C), decantation of the supernatant, and redispersion of the precipitate in water. The dispersion was dialyzed for several days with daily water changes.

Poly(NIPAm-*co*-AAc) (**Scheme S1(b)**: **NA10**) microgels were synthesized by aqueous free-radical precipitation polymerization. A mixture of NIPAm (1.511 g, 89 mol%), BIS (0.024 g, 1 mol%), AAc (0.109 g, 10 mol%) in water (90 mL) was poured in a three-necked, round-bottom flask (200 mL) which is equipped with a mechanical stirrer, condenser, and nitrogen gas inlet. The monomer solution was heated to 70 °C in an oil bath under nitrogen sparging (30 min) and constant stirring (250 rpm). After stabilization for 30 min, to initiate the polymerization, SDS (0.116 g, 4 mM) dissolved in water (5 mL) and the KPS initiator (0.054 g, 2 mM) dissolved in water (5 mL) were injected. Thereafter, stirring was continued for 4 h, the dispersion was cooled to room temperature to stop the reaction. The obtained microgels were purified by two cycles of centrifugation (415,000×g at 15 °C), decantation of the supernatant, and redispersion of the precipitate in water. The dispersion was dialyzed for several days with daily water changes.

Poly(NIPAm-*co*-AAc) (**Scheme S1(c)**: **NA30**) microgels were synthesized through aqueous free-radical precipitation polymerization. A monomer mixture of NIPAm (2.342 g, 69 mol%), BIS (0.046 g, 1 mol%), AAc (0.649 g, 30 mol%) in water (190 mL) was poured into a three-necked, round-bottom flask (300 mL) which is equipped with a mechanical stirrer, condenser, and nitrogen gas inlet. The monomer solution was heated to 70 °C in an oil bath under nitrogen sparging (30 min) and constant stirring (250 rpm). After stabilization for 30 min, to initiate the polymerization, SDS (0.288 g, 5 mM) dissolved in water (5 mL) and the KPS initiator (0.108 g, 2 mM) dissolved in water (5 mL) were added. Thereafter, stirring was continued for 4 h, the dispersion was cooled to room temperature to stop the reaction. The obtained microgels were purified by two cycles of centrifugation (415,000×g at 15 °C), decantation of the supernatant, and redispersion of the precipitate in water. The dispersion was dialyzed for several days with daily water changes.

Core/shell microgels were synthesized through seeded precipitation polymerization.[1] For that purpose, a three-necked, round-bottom flask (200 mL) equipped with a mechanical stirrer, condenser, and nitrogen gas inlet was charged with water (26 mL) and heated to 70 °C in an oil bath under nitrogen sparging (30 min) and constant stirring (250 rpm). After stabilization for 30 min, 12 mL of NA30 core microgel dispersions (1.66 wt%) and KPS initiator (0.0032 g, 2 mM) dissolved in water (2 mL) were added. After 3 min, a mixture of NIPAm (0.281 g, 99 mol%) and BIS (0.004 g, 1 mol%) in water (10 mL) were added. The reaction was allowed to proceed for 4 h, before the microgel dispersion was cooled to room temperature. The thus obtained microgels were purified by two cycles of centrifugation (415,000×g at 15 °C), decantation of the supernatant, and redispersion of the precipitate in water. The dispersion was then dialyzed for several days with

daily water changes. The D_h of the core/shell microgels detected by dynamic light scattering was 409 nm (the D_h of the NA30 core microgels was 367 nm).

Dynamic light scattering (DLS)

The hydrodynamic diameter (D_h) of the microgels in 10 mM and pH = 7 phosphate buffer (SPB) was determined by DLS (Malvern Instruments Ltd., ZetasizerNanoS). The microgel concentrations in the measurements in the range ~0.001 – 0.005 wt%. The DLS data represent averages of three individual measurements of 15 consecutive runs (30 s acquisition time of the intensity autocorrelation). Before the measurements, the samples were leaved to stand at 25 °C for 5 min to thermally equilibrate. A time-dependent scattering intensity was detected at a total scattering angle of 173°. Using the Stokes–Einstein equation, the D_h of the microgels were calculated from the measured diffusion coefficients (Zetasizer software v6.12).

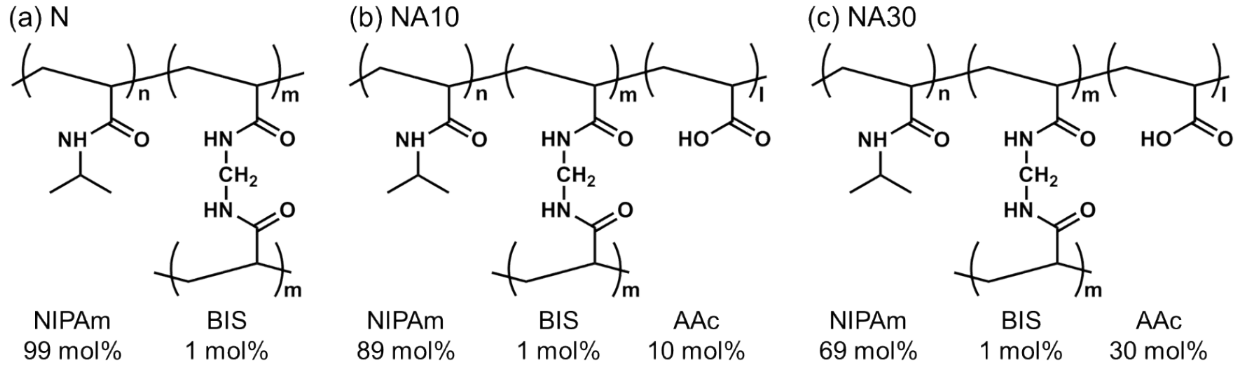

Scheme S1. Chemical structure of (a) N, (b) NA10, and (c) NA30 microgels.

Electrophoresis

The electrophoretic mobility (EPM) of the microgels in 10 mM SPB solution (pH = 7; T = 25 °C) was measured using a ZetasizerNanoZS (Malvern, Zetasizer software Ver. 4.20). The EPM of the microgels was analyzed for microgel concentrations in the range of ~0.001 – 0.005 wt%. The EPM data represent averages of three individual measurements of 20 consecutive runs. Before the measurements, the samples were leaved to stand at 25 °C for 5 min to thermally equilibrate.

Protein Assays

The amount of adsorbed protein in the microgels was estimated using the centrifugation/supernatant assay method based on the bicinconic acid (BCA) method,[2] in which proteins reduce Cu^{2+} to Cu^{+} under alkaline conditions, whereupon Cu^{+} forms complexes with BCA. The absorbance at 540 nm, which is characteristic for these complexes, allows a quantitative determination of the proteins. Protein solutions (total volume: 500 μL; [protein] = 100-1400 μg mL^{-1}) and microgel dispersions (0.01 wt%) were prepared in SPB ([SPB] = 10 mM; pH = 7; T = 25 °C), and these were mixed using a Thermomixer (Eppendolf, Thermomixer Comfort) at 1000 rpm and 25 °C for 1 h. Thereafter, the protein/microgel mixtures centrifuged (~28,000×g; T = 25 °C). From the supernatant, the protein concentration was determined via the BCA method. The absorbance at 540 nm was measured using a microplate reader (BTC, ImmunoMini NJ-2300). The adsorbed protein values represent an average of three individual measurements.

High-speed atomic force microscopy (HS-AFM)

The laboratory-built HS-AFM used in this study has been described previously.[3-4] All images and movies shown in this paper were acquired using the tapping mode, in which a cantilever (length:

6–7 μm; width: 2 μm; thickness: 90 nm) is oscillated near a mechanical resonance. The cantilever oscillation was detected by an optical-beam-deflection detector using a red laser (650 nm). Typical spring constant, resonant frequency, and quality factor values for an aqueous solution of the cantilever are ~0.1 N/m, ~600 kHz and ~2, respectively. Because the small cantilever has only a blunt bird-beak structure at the end, a sharp amorphous carbon tip was grown on the original tip by electron beam deposition. Then the carbon tip was etched to ~4 nm in radius by a RF plasma etcher under an argon atmosphere. For the HS-AFM imaging of the microgels, the cantilever free-oscillation amplitude was set to 5~30 nm, and the set-point amplitude was set to 70-90% of the free-oscillation amplitude depending on the size of microgel.

In order to adsorb the microgels onto the mica surfaces, the mica substrate was hydrophobized by fluoride resin. For that purpose, an fluoride resin (Fluoro Surf) solution (0.5 μL) was dropped on a freshly cleaved mica surface and blotted excess the solution. After natural drying the solution, 3 μL of the microgel dispersion ([microgel] = 0.05 wt%) was dropped on the hydrophobized mica substrate, and incubated for 5 min at room temperature (~25 °C). After the incubation, the substrate was rinsed with pure water to remove any excess microgels. The adsorption behavior of proteins onto the microgels on the substrates was observed by removing 8 μL from the observation solution (V = 80 μL; [SPB] = 10 mM; pH = 7) and replacing it with the same volume of a protein solution ([protein] = 1000 μg mL^{-1}) during the recording of the images. HS-AFM imaging was performed at room temperature ($T \approx 25$ °C; scanning area: 500 × 500 or 800 × 800 nm^2; 120 ×120 $pixels^2$; frame rate = 1 fps).

Results and Discussion

Table S1. Chemical composition, D_h, and EPM of the microgels measured in 10 mM SPB at pH = 7 and 25 °C.

Code	NIPAm [mol%]	BIS [mol%]	AAc [mol%]	D_h [nm]	EPM (10^{-8} $m^2V^{-1}s^{-1}$)
N	99	1	0	277	−0.31 ± 0.20
NA10	89	1	10	256	−1.83 ± 0.08
NA30	69	1	30	367	−3.71 ± 0.19

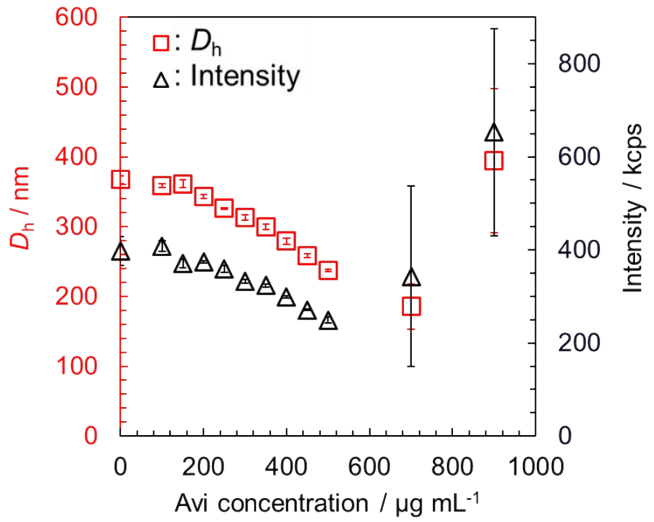

Figure S1. Avi concentration dependence of D_h and scattering intensities for the NA30 microgels detected by DLS.

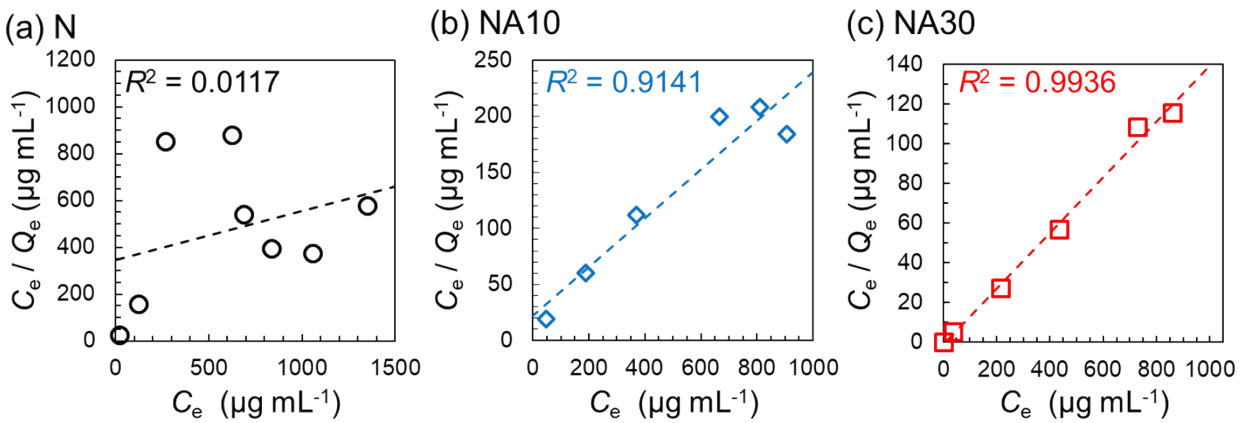

Figure S2. Langmuir isotherms for the adsorption of Avi onto microgels with different AAc contents.

The Langmuir model is based on the assumption that maximum adsorption corresponds to the formation of a monolayer of the adsorbate on the adsorbent surface according to:[5]

$$\frac{C_e}{Q_e} = \frac{C_e}{Q_m} + \frac{1}{Q_m b}$$

where C_e (μg mL^{-1}) represents the equilibrium protein concentration in solution, Q_e (g g^{-1}) the amount of protein adsorbed by the microgels, Q_m (g g^{-1}) the adsorption capacity, i.e., the amount of protein that can be absorbed by a unit mass of the adsorbent for the formation of monolayer on the surface, and b (L mg^{-1}) the Langmuir constant.

Table S2. Langmuir isotherm parameters for the adsorption of proteins onto microgels with different AAc contents obtained from the centrifugation/supernatant protein assay.

Protein	Microgel	Langmuir		
		Q_m g / g	b L / mg	R^2
LZM	N	0.4146	-0.001335	0.2973
	NA10	0.9225	0.05568	0.9477
	NA30	4.255	0.4188	0.9985
Avi	N	12.28	0.0001699	0.0117
	NA10	4.600	0.009783	0.9141
	NA30	7.128	-0.1620	0.9936
IgG	N	1.807	-0.008763	0.02132
	NA10	0.8143	-0.003202	0.1824
	NA30	4.802	0.001958	0.5215

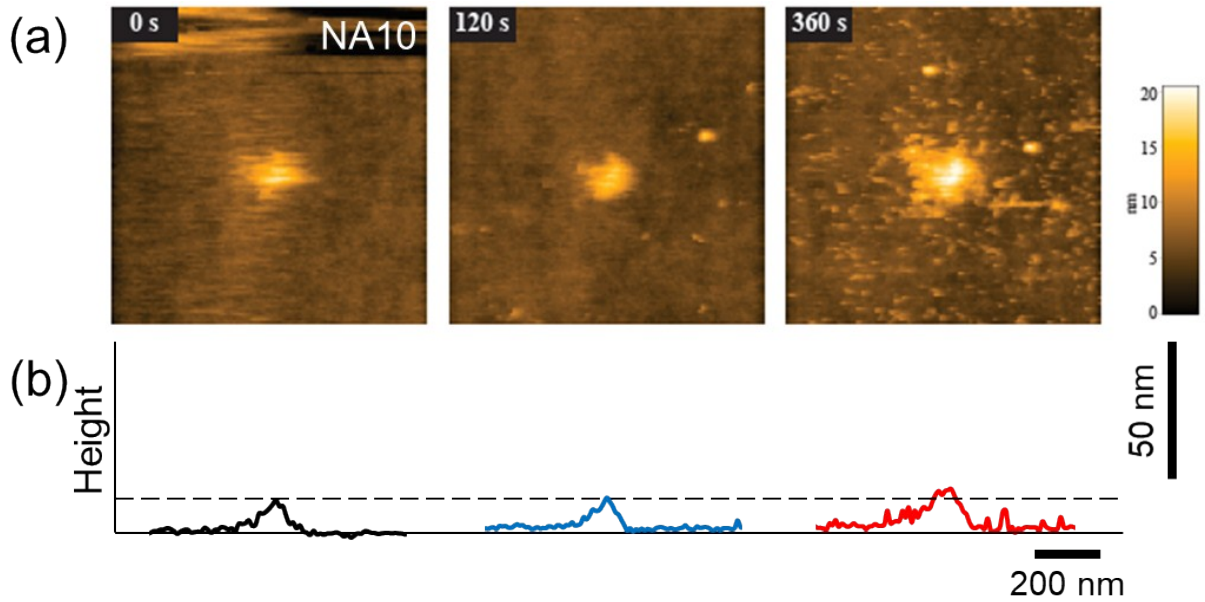

Figure S3. (a) HS-AFM images of the time-dependent adsorption of Avi onto NA10 microgels in SPB ([SPB] = 10 mM; pH = 7, T = 25 °C). Pixel: 120 × 120; scan range: 800 × 800 nm^2; frame rate: 1 fps. **(b)** Typical cross-section profiles of the NA10 microgels during Avi adsorption.

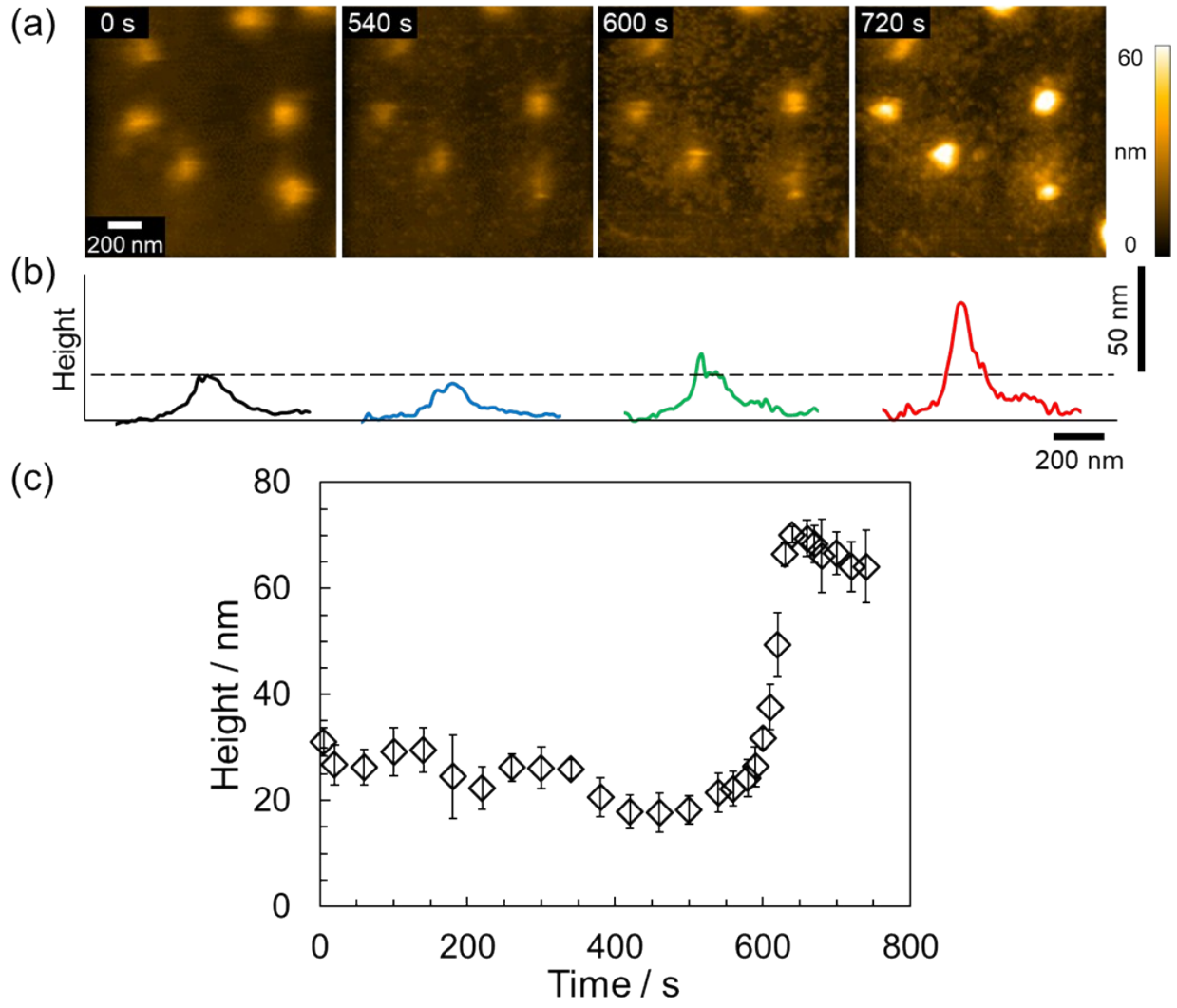

Figure S4. (a) HS-AFM images for the adsorption behavior of Avi onto the NA30 microgels in SPB solution ([SPB] = 10 mM; pH = 7; T = 25 °C; [Avi] = 100 μg mL^{-1}). Pixel: 120 × 120; scan range: 1500 × 1500 nm^2; frame rate: 1 fps. **(b)** Typical cross-section of the NA30 microgels during Avi adsorption. **(c)** Time-dependent height profiles (N = 3) for the microgels during protein adsorption.

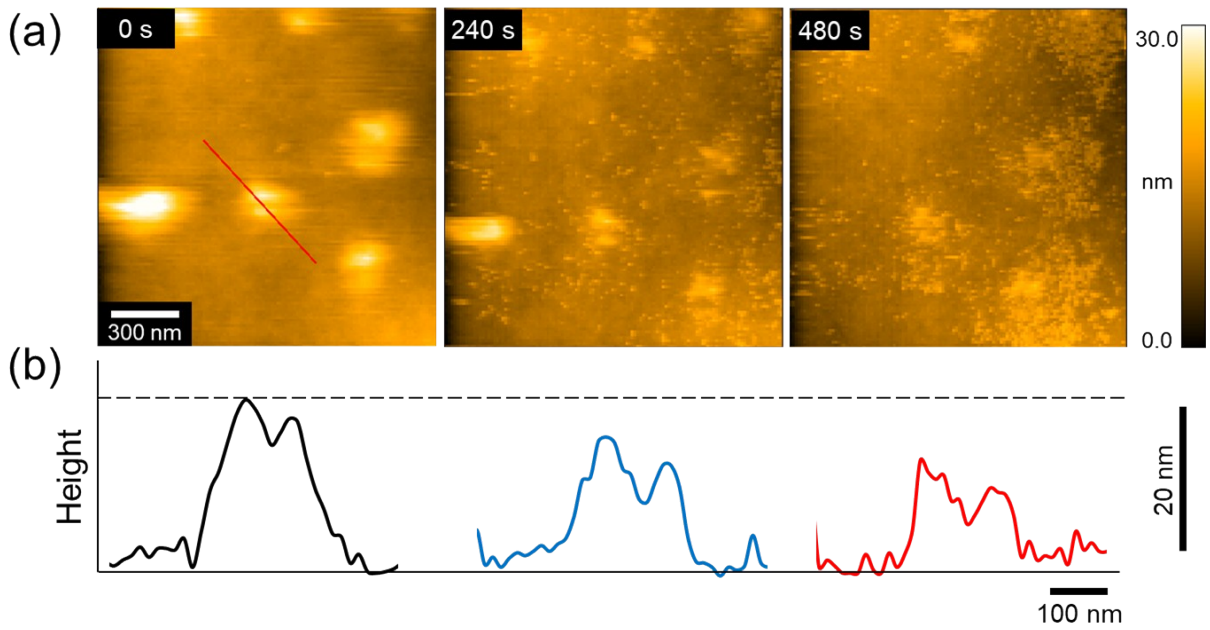

Figure S5. (a) HS-AFM images for the adsorption behavior of Avi onto the NA30 microgels in SPB solution ([SPB] = 10 mM; pH = 7; T = 25 °C; [Avi] = 10 μg mL^{-1}). Pixel: 120 × 120; scan range: 1500 × 1500 nm^2; frame rate: 1 fps. **(b)** Typical cross-section of the NA30 microgels during Avi adsorption.

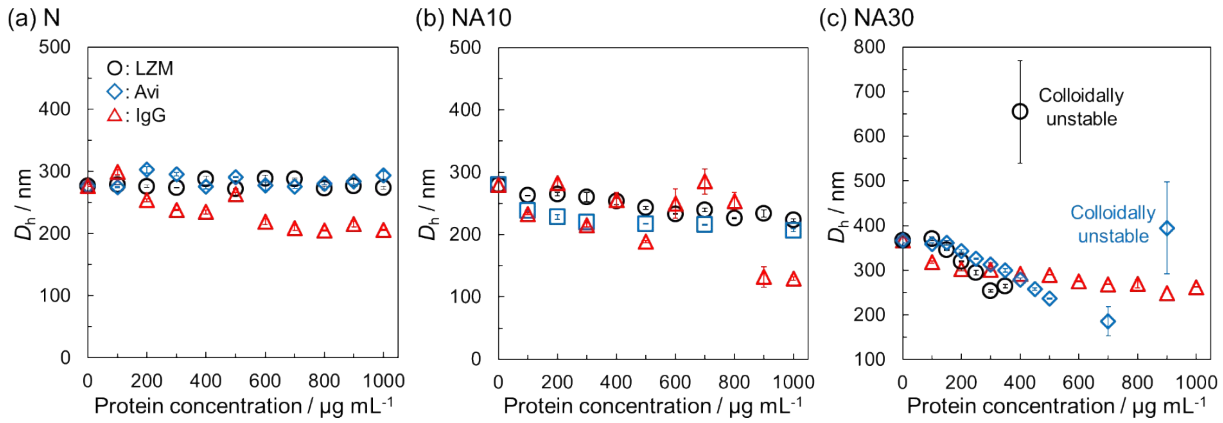

Figure S6. DLS-derived D_h values for microgels with different AAc content (**a**; N, **b**; NA10, and **c**; NA30) as a function of the protein (LZM, Avi, or IgG) concentration ([SPB] = 10 mM; pH = 7; T = 25 °C; N = 3).

To examine the effect of the protein size on the adsorption and uptake behavior, the cationic protein lysozyme (LZM; M_w = 14500; pI = 11.1~11.3; 4.5 × 3.0 × 3.0 nm),[6] which is smaller than Avi, and immunoglobulin G (IgG; M_w = 150000; pI = 9.0; 14.5 × 8.5 × 4.0 nm),[7] which is larger than Avi, were investigated. The D_h of the microgels as a function of the protein concentration. In the case of the weakly charged N and NA10 microgels, no obvious differences in the changes in the D_h were observed depending on the protein type (LZM and Avi) (**Figure S6ab**). In the presence of LZM, the D_h of the NA30 microgels decreased from D_h = 367 (LZM: 0 μg mL^{-1}) to D_h = 254 nm (LZM: 300 μg mL^{-1}) before aggregation of the microgels was observed at a lower concentration (>400 μg mL^{-1}) than for Avi (**Figure S6c**). Conversely, in the presence of IgG, the D_h of the NA30 microgels only gradually decreased from D_h = 367 nm (IgG: 0 μg mL^{-1}) to D_h = 262 nm (IgG: 1000 μg mL^{-1}) (**Figure S6c**).

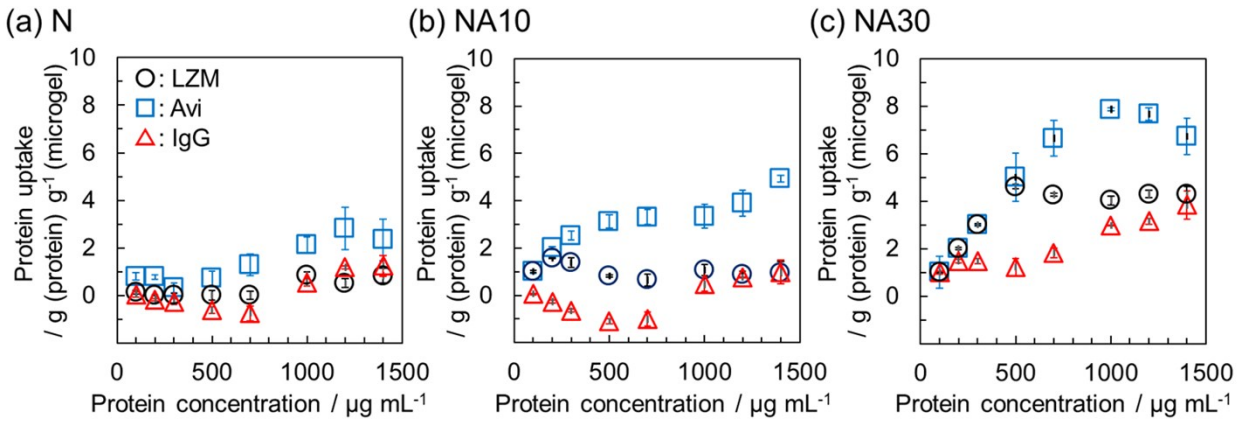

Figure S7. Protein (LZM, Avi and IgG) uptake per unit mass of (**a**) N, (**b**) NA10, and (**c**) NA30 microgels as a function of the protein concentration determined using the centrifugation/supernatant protein assay ([SPB] = 10 mM; pH = 7; T = 25 °C).

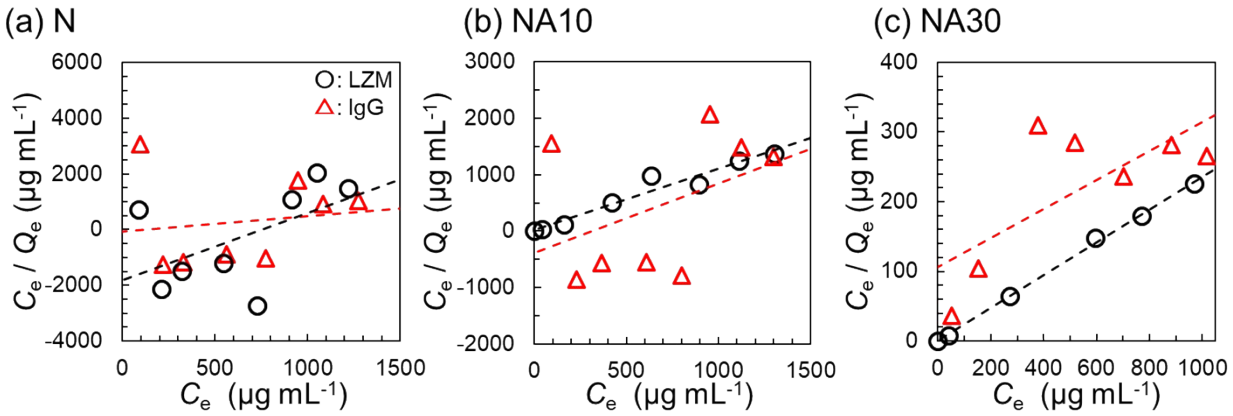

Figure S8. Langmuir isotherms for the adsorption of proteins (LZM and IgG) onto microgels with different AAc contents.

Similar to the Avi uptake, the adsorption isotherms of these proteins onto the N microgels could not be fitted using the Langmuir model (**Figure S8a**). Conversely, the adsorption isotherm of LZM to the NA10 and NA30 microgels was a good fit for the Langmuir model (**Figure S8bc**). The saturation uptake of LZM without aggregation of the microgels ([LZM] = 300 μg mL^{-1}) was 3.0 g g^{-1} (corresponding to ~7.4 × 10^4 LZM per sphere), which is higher than that for Avi probably due to the smaller size of LZM relative to Avi. In contrast, the adsorption isotherm for IgG could not be fitted using the Langmuir model (**Figure S8c**). The uptake of IgG in the NA30 microgels was 1.5 g g^{-1} at [IgG] = 300 μg mL^{-1} (corresponding to ~3.5 × 10^3 IgG per a sphere), which is much lower than that for Avi and LZM. The occupied area of IgG for the NA30 microgel surface was determined (~5.8 × 10^5 nm^2) to be comparable to that of the microgel surface area (~4.2 × 10^5 nm^2). These results indicate that IgG should not penetrate the microgels but almost molecules of IgG should adsorb onto the microgel surface due to the size exclusion effect.

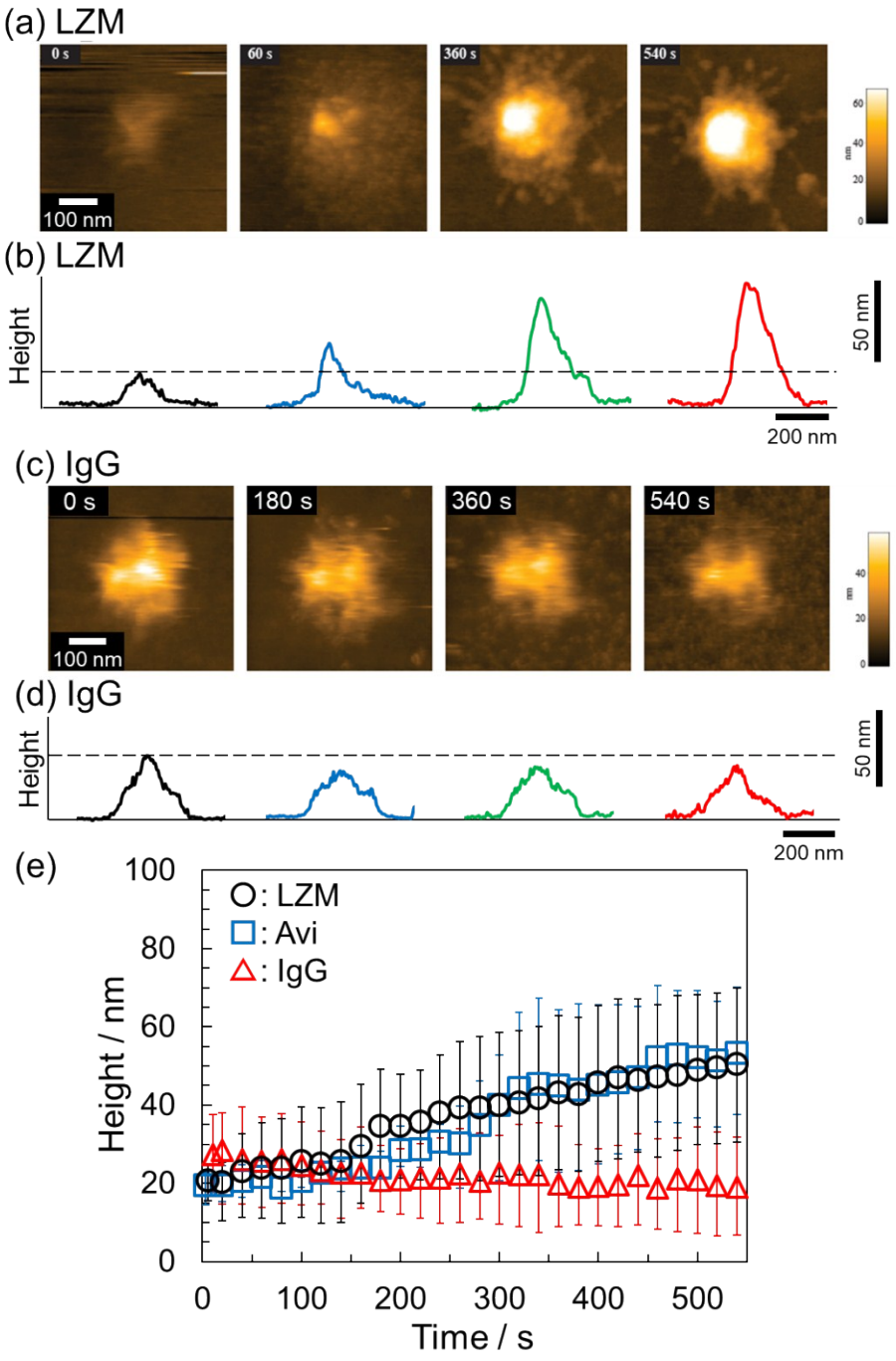

Figure S9. HS-AFM images for the time-dependent adsorption of **(a)** LZM and **(c)** IgG onto the NA30 microgels in SPB ([SPB] = 10 mM, pH = 7; T = 25 °C). Pixel: 120 × 120; scan range: 500 × 500 nm^2; frame rate: 1 fps. Typical cross-section profiles for the NA30 microgels during the

adsorption of **(b)** LZM and **(d)** IgG. Time-dependent height profiles (N = 3) for the microgels during protein adsorption.

The adsorption and uptake processes of LZM and IgG were also observed by HS-AFM. After the injection of an LZM solution into the solution pool, a gradual increase of the NA30 microgel height from h = 21 nm (0 s) to h = 49 nm (500 s) was observed, which suggests that LZM molecules are adsorbed onto the NA30 microgels with multi-layer adsorption (**Movie S2a** and **Figure S9abe**). This adsorption behavior of LZM is similar to the adsorption of Avi (**Figure 2cd**). However, in the case of IgG, the NA30 microgel slightly collapsed as seen in the morphology and height (h = 27 nm at 0 s; h = 21 nm at 500 s), which is consistent with the DLS data, and excessive superficial layers of IgG were not observed during the adsorption of IgG (**Movie S2b** and **Figure S9cde**). These results suggest that IgG is unable to intrude into the microgel network due to the size exclusion effect. Taken together, we assume that the penetration of proteins into the microgels and the saturation with the proteins induce the formation of excessive protein layers on the surface of the microgels and their aggregation in solution.

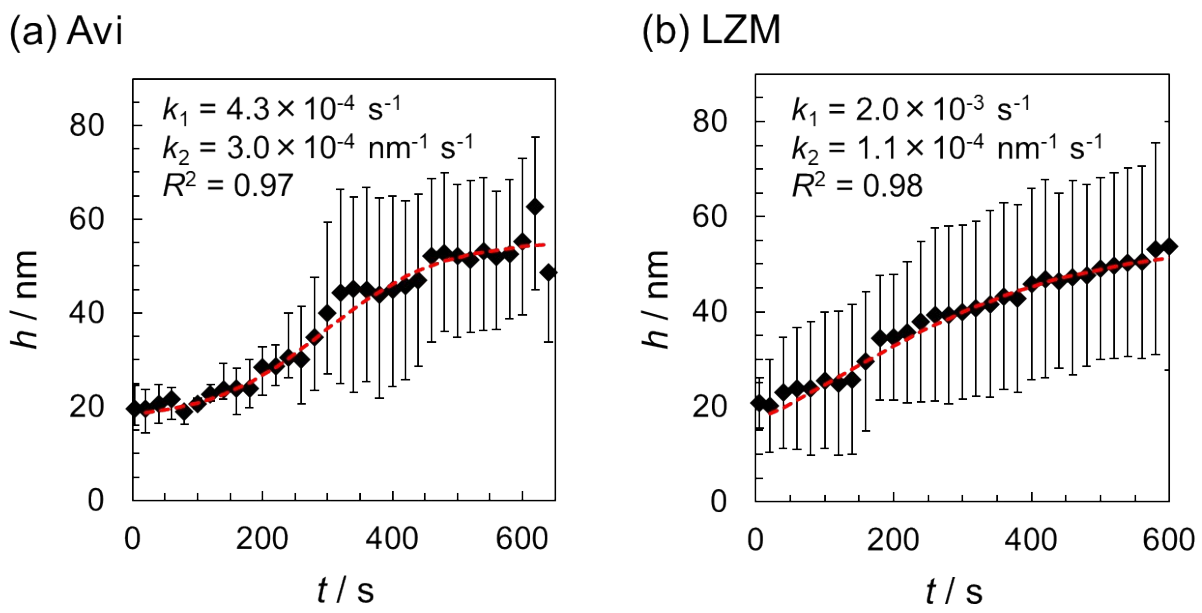

Figure S10. Time-dependent height profiles (N = 3) of NA30 microgels during the adsorption of (a) Avi and (b) LZM. The dotted red lines are the fitting curves based on the fitted by the following Finke-Watzky model.[8] The obtained rate constants are (a) $k_1 = 4.3\times10^{-4}$ s^{-1} and $k_2 = 3.0\times10^{-4}$ nm^{-1} s^{-1} (R^2 = 0.97) (b) $k_1 = 2.0\times10^{-3}$ s^{-1} and $k_2 = 1.1\times10^{-4}$ nm^{-1} s^{-1} (R^2 = 0.98), respectively.

$$h_t = h_0\left(1 - \frac{k_1 + k_2 h_0}{k_2 h_0 + k_1 \cdot e^{(k_1 + k_2 h_0)t}}\right)$$

where h_t (nm) represents the height change of microgels on a substrate at time, t, h_0 (nm) denominates the height at equilibrium time (~600 s), and k_1 and k_2 represent the nucleation and growth rate constant, respectively.

Supporting Movies

Movie S1. HS-AFM movies for the adsorption behavior of Avi onto microgels with different AAc content (30× speed): **(a)** N and **(b)** NA30.

Movie S2. HS-AFM movies for the adsorption behavior of LZM and IgG onto NA30 microgels (30× speed): **(a)** LZM and **(b)** IgG.

Movie S3. HS-AFM movies for the adsorption of LZM onto core/shell microgels (30× speed).

References

1. C. D. Jones, L. A. Lyon, *Macromolecules*, 2000, **33**, 8301–8306.
2. C.M. Stoscheck, *Methods Enzymol*, 1990, **182**, 50–68.
3. T. Ando, T. Uchihashi, S. Scheuring, *Chem. Rev.*, 2014, **114**, 3120–3188.
4. S. Matsui, T. Kureha, S. Hiroshige, M. Shibata, T. Uchihashi, D. Suzuki, *Angew. Chem., Int. Ed.*, 2017, **56**, 12146–12149.
5. I. Langmuir, *J. Am. Chem. Soc.*, 1917, **39**, 1848−1906.
6. W. C. K. Poon, S. U. Egelhaaf, P. A. Beales, A. Salonen, L. Sawyer, *J. Phys. Condens. Matter*, 2000, **12**, L569.
7. Y. H. Tan, M. Liu, B. Nolting, J. G. Go, J. Gervay-Hague, G. Liu, *ACS Nano*, 2008, **2**, 2374–2384.
8. (a) M. A. Watzky, R. G. Finke, *J. Am. Chem. Soc.*1997, **119**, 10382–10400; (b) A. M. Morris, M. A. Watzky, R. G. Finke, *Biochim. Biophys. Acta Proteins Proteomics* 2009, **1794**, 375–397; (c) T. Fukui, S. Kawai, S. Fujinuma,Y. Matsushita, T. Yasuda, T. Sakurai, S. Seki, M. Takeuchi, K. Sugiyasu, *Nat. Chem.* 2017, **9**, 493–499.